PROCEEDINGS OF SPIE

Molecular doping of single-walled carbon nanotube transistors: optoelectronic study

Jiangbin Zhang
Aleksei V. Emelianov
Artem A. Bakulin
Ivan I. Bobrinetskiy

SPIE.

Molecular doping of single-walled carbon nanotube transistors: optoelectronic study

Jiangbin Zhang[a], Aleksei V. Emelianov[b], Artem A. Bakulin*[a,c], Ivan I. Bobrinetskiy[b]

[a]Cavendish Laboratory, University of Cambridge, J J Thomson Avenue, Cambridge, CB3 0HE, UK;
[b]National Research University of Electronic Technology, Moscow, 124498, Russia;
[c]Department of Chemistry, Imperial College London, London, SW7 2AZ, UK;

ABSTRACT

Single-walled carbon nanotubes (SWCNT) are a promising material for future optoelectronic applications, including flexible electrodes and field-effect transistors. Molecular doping of carbon nanotube surface can be an effective way to control the electronic structure and charge dynamics of these material systems. Herein, two organic semiconductors with different energy level alignment in respect to SWCNT are used to dope the channel of the SWCNT-based transistor. The effects of doping on the device performance are studied with a set of optoelectronic measurements. For the studied system, we observed an opposite change in photo-resistance, depending on the type (electron donor vs electron acceptor) of the dopants. We attribute this effect to interplay between two effects: (i) the change in the carrier concentration and (ii) the formation of trapping states at the SWCNT surface. We also observed a modest ~4 pA photocurrent generation in the doped systems, which indicates that the studied system could be used as a platform for multi-pulse optoelectronic experiments with photocurrent detection.

Keywords: single-walled carbon nanotube; organic semiconductor; photocurrent generation; chemical vapor deposition.

1. INTRODUCTION

Due to the unique electronic properties of single-walled carbon nanotubes (SWCNT)[1–3], these quasi-one-dimensional materials have been widely investigated and applied in various device systems, such as field effect transistors (FET)[4], optical switches[5], organic photovoltaics (OPV)[6] and organic light emitting diodes (OLED)[7]. Charge dynamics at the interface between SWCNT and organic molecules/metals is of particular importance for the fundamental understanding of carbon-based electronic materials as well as for the development of new types of devices in organic electronics. One recent example is the observation of Marcus inverted region in SWCNT heterojunction[8]. To resolve the charge dynamics of SWCNT-based systems, ultrafast optical spectroscopy[8–12] is being widely applied. This method becomes an important tool to undercover various ultrafast dynamics, such as exciton dissociation[6,8], recombination[13], relaxation[14], multi-exciton generation[10], and charge transfer[15].

The potential of SWCNT materials for flexible electronic devices comes from the fact that they can be used both as the channel material in FETs and as the transparent and conductive electrodes[16]. For example, in organic solar cell, SWCNT film/plastic anode has showed better performance on flexibility and environmental advantage over indium tin oxide (ITO)/glass with a similar efficiency[17,18]. In the FET configuration, SWCNTs can also be used as electrodes for robust and versatile molecular junctions[19].

Molecular doping is one possible way to modify the electronic properties of the SWCNTs. Due to the energy level difference, charge transfer (electron transfer or hole transfer) can happen at the interface between SWCNT and organic molecules, which would lead to the change in the electronic structure of SWCNT as well as in the concertation of mobile carriers. In this paper, we perform several optoelectronic experiments to observe the charge transfer and charge generation in our studied system.

1.1 Material

A,a'-dihexylquaterthiophene (LY106) is a p-type semiconductor and the highest occupied molecular orbital (HOMO) energy level is -5.2 eV. It acts as the acceptor while SWCNT acts as the donor. Perylenetetracarboxylicdianhydride (PTCDA) is an electron-donating semiconductor and the HOMO and lowest unoccupied molecular orbital (LUMO) energy levels are -6.8 eV and -4.7 eV, respectively. It can act as donor in the PTCDA/SWCNT interface. The molecular

structures are shown below. Materials were received from Sigma Aldrich, USA (PTCDA) and provided by Institute of Synthetic Polymer Materials, Russia (LY106).
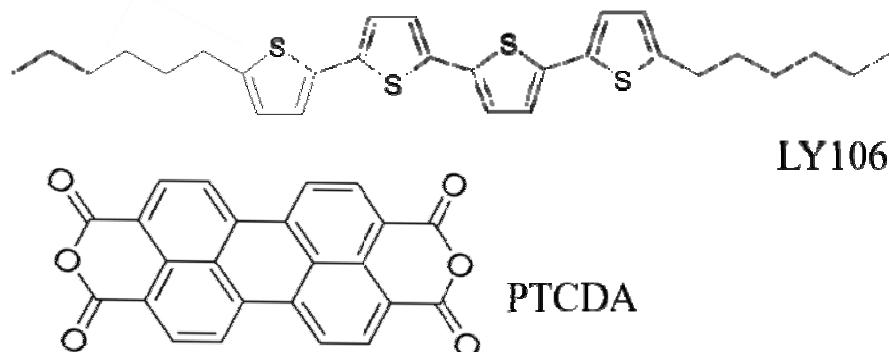

Figure 1.1 Molecular structures of LY106 and PTCDA.

1.2 Device fabrication

SWCNTs (provided by Professor A. Nasibulin, Skoltech) were deposited on Si/SiO$_2$ substrate using gas-phase process formation based on thermal decomposition of ferrocene in the presence of carbon monoxide[20]. Source and drain (100/5 nm Au/Ti) electrodes were fabricated by photolithography, and the gate electrode was highly doped (p^{++}) Si substrate. As shown in Figure 1.2 (A), a thin layer of organic molecules (LY106 and PTCDA) was evaporated in vacuum (10^{-4} Pa) onto the small area with the specific thickness of 5 nm and 2 nm, respectively. The amount of SWCNTs and the device morphology were determined by atomic-force microscopy (AFM) and scanning electron microscopy (SEM). Figure 1.2 (B) represents a typical SWCNT FET structure with certain amount of nanotubes. The gap between electrodes was 1.5 μm. Figure 1.2 (C) shows the topography after the deposition of LY106 molecules. The film consists of clusters of 5-10 nm average height, which covers SWCNTs between electrodes.
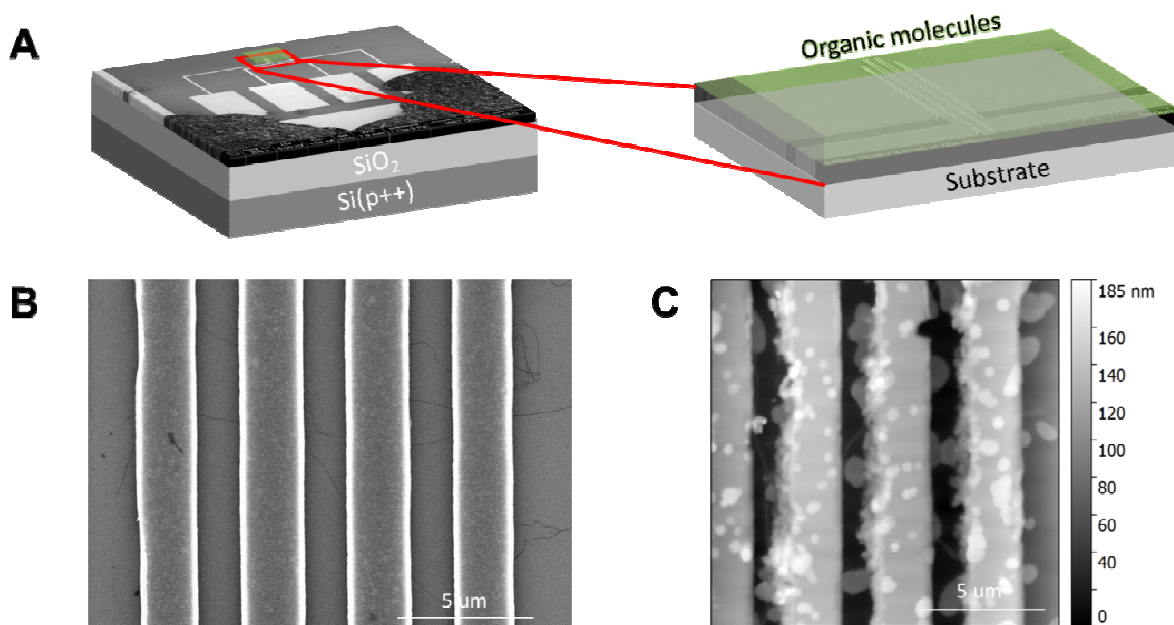

Figure 1.2 (A) Left panel: device structure with different layers on SiO$_2$/Si substrate; right panel: magnified area where the organic molecules are deposited; (B) SEM image of pristine SWCNTs between gold electrodes; the gap between the adjacent electrodes was 1.5 μm; (C) AFM image of SWCNTs coated with LY106 molecules.

1.3 Electrical measurement

All SWCNT structures were measured before and after the deposition of molecules through a semiconductor parameter analyzer (MNIPI, Belarus) under normal conditions. To prevent the damage due to the high value of current density in the channel and at the contacts we limit the drain current down to 300 nA.

1.4 Optoelectronic measurement

Figure 1.3 (A) shows the setup for measuring the effect of light on current-voltage (I-V) curve of the devices. The dark conductivity was directly measured by Keithley 2400 under room light. To measure the photo-conductivity, the laser diode at 405 nm (CPS 405, Thorlabs) was focused on the sample area of around 0.5 mm^2 and the power was reduced by neutral density filter to several μW.

Figure 1.3 (B) shows the schematic to measure photocurrent generation in the device. The laser light was modulated by the chopper (MC2000, Thorlabs), which was synchronized to the lock-in amplifier (LIA, SR 830, Stanford Research System) as the reference frequency. The sample was biased by an adjustable voltage and the influence of light on the sample was detected by the LIA.
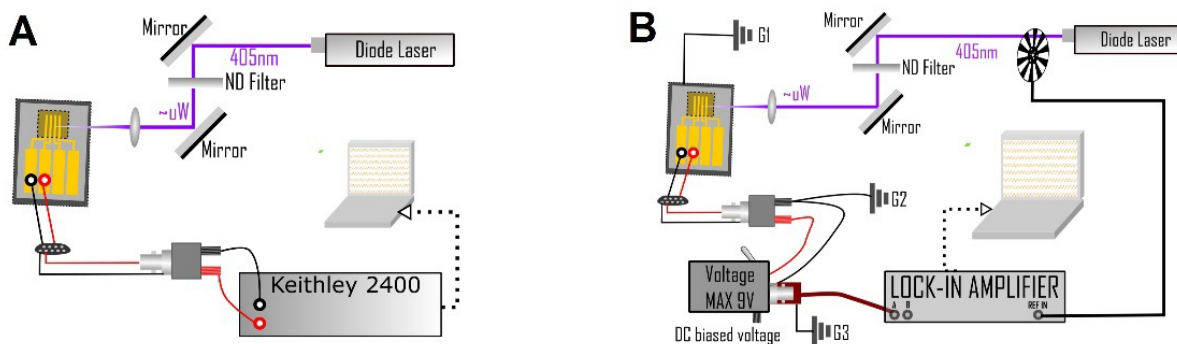

Figure 1.3 (A) Setup for measuring the effect of light on device I-V curve; (B) Setup for measuring the photocurrent generation;ND: neutral density; G: ground.

2. RESULTS AND DISCUSSION

2.1 Electrical characterization

Typical output and transfer I-V curves before and after LY106 and PTCDA deposition are shown in Figure 2.1. While the output I-V characteristics are remained, the transfer curves are drastically changed after the coating. When SWCNTs are coated with a thin molecular layer the Fermi level of the nanotubes is shifted. For SWCNTs with LY106 molecules, the Fermi level is shifted closer to the valance band and the transconductance is drastically increased. For the nanotubes with PTCDA film, the Fermi level is shifted closer to the conduction band and we do not observe any field effect anymore. This indicates that the doping switches off the transistor behavior of all the semiconducting nanotubes. Thus, all the changes we attribute to the doping effect from coated molecules, which modifies the SWCNT energy structure[21].

2.2 Optoelectronic Characterization

In order to see how the molecular doping affects the optoelectronic properties of the SWCNT, two types of experiments described in the part 1.4 were performed on the transistors.

Figure 2. shows the photocurrent generation (Figure 1.3A) in the PTCDA-deposited device. The 405nm light modulated at 370 Hz was blocked and unblocked every 15 seconds and the change in current was recorded with LIA. From the left panel (grey), the background noise level was ~1 pA while from the right panel (white), the photocurrent was ~5 pA. The small but present ~4 pA photocurrent proves the possibility of photocurrent generation in the PTCDA-deposited device. This photocurrent most likely originates from the photoexcitation of PTCDA. Immediately after the exciton formation,

electron transfer is expected to occur from PTCDA to SWCNTs. The photogenerated mobile carriers are later collected by the electrodes under the 100 mV bias.
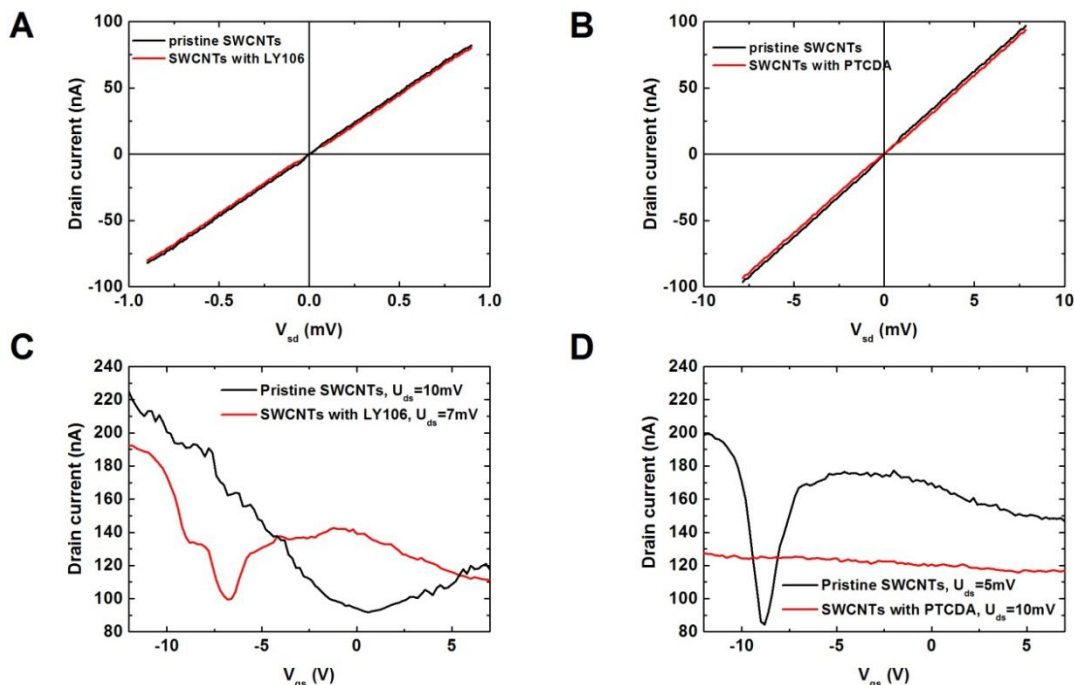

Figure 2.1 (A) Output I-V curves for pristine and coated SWCNTs with LY106 molecules; (B) Output I-V curves for pristine and coated SWCNTs with PTCDA molecules; (C) Transfer I-V curves for pristine and coated SWCNTs with LY106 molecules; (D) Transfer I-V curves for pristine and coated SWCNTs with PTCDA molecules.
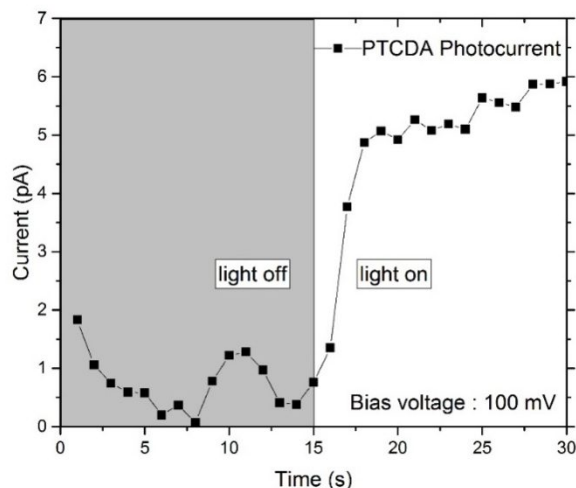

Figure 2.2 Photocurrent of the SWCNT device deposited by PTCDA under the direct-current voltage of 100 mV. The light was modulated by the optical chopper at 370 Hz and the current was detected with LIA.

In order to further resolve the charge dynamics in these devices, the conductivity change under the light illumination was investigated (Figure 1.3B). Figure 2. shows the change of the I-V curve under the illumination of 405 nm laser light for different dopants. For LY106 (Figure 2.A), the black curve was measured under room light. When the laser light is on, a steeper curve (blue) was observed, which indicates towards a higher conductivity. When the power increased from 10 μW to 30 μW, these two I-V curves overlapped with each other, which indicates the presence of the saturation effect. For PTCDA (Figure 2.B), the conductivity was reduced under light illumination, which is different from LY106. In both

samples, we found that the recovery process from the 'under-light' conductivity to the 'dark' conductivity was much slower than the photo-doping process. This is clearly illustrated in Figure 2.C, which shows the conductivity/resistance change of PTCDA after the laser was blocked.
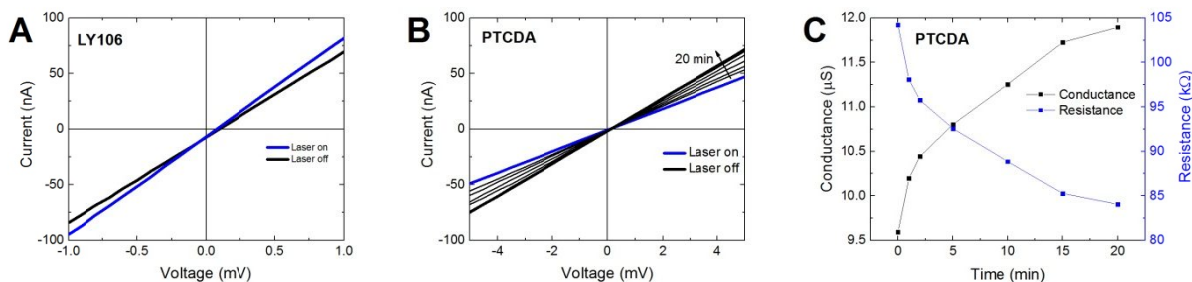

Figure 2.3 The photo-induced effect on the I-V curve. (A) I-V curve of the LY106-deposited device without laser illumination and with laser illumination at 10 µW; (B) I-V curves of the PTCDA-deposited device, blue line is under laser illumination and the black curves show the change up to 20 min after blocking the laser light; (C) Resistance and conductance change over time after illumination was blocked.

Plasmon generation in SWCNT should not dominate this process as it has a much faster response time. The possible change would come from the conductivity, which is determined by the majority carrier concentration and its mobility,

$$\sigma = q(\mu_n n + \mu_p p) \tag{1}$$

where μ_n and μ_p refer to the mobilities of electrons and holes, and n and p refer to the number of electrons and holes, respectively. If the mobility causes this change, conductivity change should happen very fast. Therefore, the change of conductivity probably comes from the change of the concentration.

Considering the energy offsets of HOMO and LUMO energy levels at the interface (Figure 2.4), we propose an explanation to the observed effects based on interplay between two phenomena. Under the illumination, excitons can be generated in the molecular dopants (PTCDA or LY106). In PTCDA system, the small LUMO offset would induce electron transfer to SWCNT, while for LY106, hole transfer should be favorable at the interface. As the SWCNT is a p-type semiconductor under normal conditions, the majority carriers are the holes. Electron (hole) transfer from PTCDA (LY106) would decrease (increase) the hole concentration, which can explain the increase of the conductivity under illumination. However, the charge carriers remaining on the dopant molecules are likely to be immobile. Their presence can prevent further charge transfer process, and they may also serve as trapping sites for the mobile carriers in SWCNTs. It is most likely that trapped hole left on PTCDA have a stronger negative effect on the SWCNT carrier mobilities. When the laser illumination is blocked, the concentration and distribution of carriers slowly return to their original level due to charge diffusion and recombination.
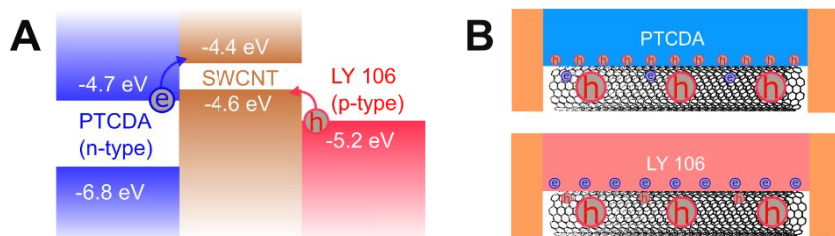

Figure 2.4 Mechanism of photo-induced effect. (A) The HOMO and LUMO energy levels of PTCDA, SWCNT and LY106. Electron (hole) transfer would happen between the interface of PTCDA (LY106) and SWCNT. (B) Diagram shows that the electron (hole) transfer from PTCDA (LY106), which decreases (increases) the hole concentration.

The observation of the photocurrent generation shows the possibility of investigating excitonic behaviors in these devices.

Currently, we still cannot completely exclude the influence of SWCNT exciton generation. Laser sources at higher wavelengths would be chosen to excite the sample in the following experiments. Another possibility of the result of molecular doping would be the formation of the intermolecular complex[22], like charge transfer states in organic solar cells. However, simple quasi-steady state optoelectronic experiments cannot detect these states. To discriminate this possibility and to see whether some trap states are formed, the novel pump-push spectroscopy will be applied in the future.

3. CONCLUSIONS

In this study, we have performed both electrical and optoelectronic measurement of the SWCNT devices, which are doped with an additional layer of organic molecules. Electrical measurements before and after molecules deposition show a substantial change in transfer I-V characteristics due to molecules doping. LY106 molecules shift the Fermi level of SWCNTs closer to the valence band increasing the hole concentration and transconductance, while PTCDA molecules drastically decrease the number of holes, shifting the Fermi level closer to the conduction band. In the optoelectronic measurement, ~4 pA photocurrent generation was observed in modulation light, which we associate with the charge transfer from organic molecules to SWCNTs. To further watch the doping effect, the light effect on the I-V curves were measured. For electron-donating material, like PTCDA, electron transfer to SWCNT leads to the lower conductivity of SWCNT while hole transfer from LY106 increases the hole concentration and thus the conductivity. On the other hand, the recovering process of I-V curve without illumination, due to charge diffusion and recombination, happens in a much slower speed than the photo doping process. We anticipate the optoelectronic systems similar to those studied in this work can be used for ultrafast experiments with photocurrent detection[23].

ACKNOWLEDGEMENT

REFERENCES

[1]   Avouris, P. and Chen, J., "Nanotube electronics and optoelectronics," Mater. Today **9**(10), 46–54 (2006).
[2]   Avouris, P., Freitag, M. and Perebeinos, V., "Carbon-nanotube photonics and optoelectronics," Nat. Photonics **2**(6), 341–350 (2008).
[3]   Du, J., Pei, S., Ma, L. and Cheng, H. M., "25th anniversary article: Carbon nanotube- and graphene-based transparent conductive films for optoelectronic devices," Adv. Mater. **26**(13), 1958–1991 (2014).
[4]   Dekker, C., Tans, S. J. and Verschueren, A. R. M., "Room-temperature transistor based on a single carbon nanotube," Nature **393**(6680), 49–52 (1998).
[5]   Nienhaus, L., Wieghold, S., Nguyen, D., Lyding, J. W., Scott, G. E. and Gruebele, M., "Optoelectronic Switching of a Carbon Nanotube Chiral Junction Imaged with Nanometer Spatial Resolution," ACS Nano **9**(11), 10563–10570 (2015).
[6]   Dowgiallo, A.-M., Mistry, K. S., Johnson, J. C., Reid, O. G. and Blackburn, J. L., "Probing Exciton Diffusion and Dissociation in Single-Walled Carbon Nanotube–C $_{60}$ Heterojunctions," J. Phys. Chem. Lett. **7**(10), 1794–1799 (2016).
[7]   Zhang, M., Fang, S., Zakhidov, A. A., Lee, S. B., Aliev, A. E., Williams, C. D., Atkinson, K. R. and Baughman, R. H., "Strong, transparent, multifunctional, carbon nanotube sheets," Science **309**(5738), 1215–1219 (2005).
[8]   Ihly, R., Mistry, K. S., Ferguson, A. J., Clikeman, T. T., Larson, B. W., Reid, O., Boltalina, O. V., Strauss, S. H., Rumbles, G. and Blackburn, J. L., "Tuning the driving force for exciton dissociation in single-walled carbon nanotube heterojunctions," Nat. Chem. **8**(April), 1–7 (2016).
[9]   Jensen, S. A., Ulbricht, R., Narita, A., Feng, X., Müllen, K., Hertel, T., Turchinovich, D. and Bonn, M., "Ultrafast photoconductivity of graphene nanoribbons and carbon nanotubes," Nano Lett. **13**(12), 5925–5930 (2013).
[10]   Wang, S., Khafizov, M., Tu, X., Zheng, M. and Krauss, T. D., "Multiple exciton generation in single-walled

carbon nanotubes," Nano Lett. **10**(7), 2381–2386 (2010).

[11] Reich, S., Dworzak, M., Hoffmann, A., Thomsen, C. and Strano, M. S., "Excited-state carrier lifetime in single-walled carbon nanotubes," Phys. Rev. B **71**(3), 033402 (2005).

[12] Varene, E., Bogner, L., Bronner, C. and Tegeder, P., "Ultrafast exciton population, relaxation, and decay dynamics in thin oligothiophene films," Phys. Rev. Lett. **109**(20), 1–5 (2012).

[13] Lauret, J.-S., Voisin, C., Cassabois, G., Delalande, C., Roussignol, P., Jost, O. and Capes, L., "Ultrafast carrier dynamics in single-wall carbon nanotubes.," Phys. Rev. Lett. **90**(5), 057404 (2003).

[14] Manzoni, C., Gambetta, A., Menna, E., Meneghetti, M., Lanzani, G. and Cerullo, G., "Intersubband Exciton Relaxation Dynamics in Single-Walled Carbon Nanotubes," Phys. Rev. Lett. **94**(20), 207401 (2005).

[15] Eklund, P. C., Rao, A. M., Bandow, S., Thess, A. and Smalley, R. E., "Evidence for charge transfer in doped carbon nanotube bundles from Raman scattering," Nature **388**(6639), 257–259 (1997).

[16] Park, S., Vosguerichian, M. and Bao, Z., "A review of fabrication and applications of carbon nanotube film-based flexible electronics," Nanoscale **5**(5), 1727 (2013).

[17] Rowell, M. W., Topinka, M. A., McGehee, M. D., Prall, H.-J., Dennler, G., Sariciftci, N. S., Hu, L. and Gruner, G., "Organic solar cells with carbon nanotube network electrodes," Appl. Phys. Lett. **88**(23), 233506 (2006).

[18] Jeon, I., Cui, K., Chiba, T., Anisimov, A., Nasibulin, A. G., Kauppinen, E. I., Maruyama, S. and Matsuo, Y., "Direct and Dry Deposited Single-Walled Carbon Nanotube Films Doped with MoO$_x$ as Electron-Blocking Transparent Electrodes for Flexible Organic Solar Cells," J. Am. Chem. Soc. **137**(25), 7982–7985 (2015).

[19] Jia, C., Ma, B., Xin, N. and Guo, X., "Carbon Electrode-Molecule Junctions: A Reliable Platform for Molecular Electronics," Acc. Chem. Res. **48**(9), 2565–2575 (2015).

[20] Moisala, A., Nasibulin, A. G., Brown, D. P., Jiang, H., Khriachtchev, L. and Kauppinen, E. I., "Single-walled carbon nanotube synthesis using ferrocene and iron pentacarbonyl in a laminar flow reactor," Chem. Eng. Sci. **61**(13), 4393–4402 (2006).

[21] Bobrinetskiy, I. I., Emelianov, A. V., Nevolin, V. K. and Romashkin, A. V., "Effect of an organic molecular coating on control over the conductance of carbon nanotube channel," Semiconductors **48**(13), 1735–1741 (2014).

[22] Méndez, H., Heimel, G., Opitz, A., Sauer, K., Barkowski, P., Oehzelt, M., Soeda, J., Okamoto, T., Takeya, J., Arlin, J.-B., Balandier, J.-Y., Geerts, Y., Koch, N. and Salzmann, I., "Doping of Organic Semiconductors: Impact of Dopant Strength and Electronic Coupling," Angew. Chemie Int. Ed. **52**(30), 7751–7755 (2013).

[23] Bakulin, A. A., Silva, C. and Vella, E., "Ultrafast Spectroscopy with Photocurrent Detection: Watching Excitonic Optoelectronic Systems at Work," J. Phys. Chem. Lett. **7**(2), 250–258 (2015).